Signal Processing 108 (2015) 509–520

Contents lists available at ScienceDirect

Signal Processing

journal homepage: www.elsevier.com/locate/sigpro

Steady-state performance of multimodulus blind equalizers

Ali W. Azim [a,b], Shafayat Abrar [b,*], Azzedine Zerguine [c], Asoke K. Nandi [d]

[a] Institute Polytechnique de Grenoble Saint Martin d'Hères 38400, France
[b] COMSATS Institute of Information Technology, Islamabad 44000, Pakistan
[c] King Fahd University of Petroleum & Minerals, Dhahran 31261, Saudi Arabia
[d] Brunel University, Uxbridge, Middlesex UB8 3PH, UK

ARTICLE INFO

Article history:
Received 8 July 2014
Received in revised form
16 September 2014
Accepted 14 October 2014
Available online 23 October 2014

Keywords:
Blind equalization
Multimodulus algorithm
Mean square error
Tracking performance
Steady-state analysis
Quadrature amplitude modulation
Energy conservation theorem
Variance relation

ABSTRACT

Multimodulus algorithms (MMA) based adaptive blind equalizers mitigate inter-symbol interference in a digital communication system by minimizing dispersion in the quadrature components of the equalized sequence in a decoupled manner, i.e., the in-phase and quadrature components of the equalized sequence are used to minimize dispersion in the respective components of the received signal. These unsupervised equalizers are mostly incorporated in bandwidth-efficient digital receivers (wired, wireless or optical) which rely on quadrature amplitude modulation based signaling. These equalizers are equipped with nonlinear error-functions in their update expressions which makes it a challenging task to evaluate analytically their steady-state performance. However, exploiting variance relation theorem, researchers have recently been able to report approximate expressions for steady-state excess mean square error (EMSE) of such equalizers for noiseless but interfering environment.

In this work, in contrast to existing results, we present exact steady-state tracking analysis of two multimodulus equalizers in a non-stationary environment. Specifically, we evaluate expressions for steady-state EMSE of two equalizers, namely the MMA2-2 and the βMMA. The accuracy of the derived analytical results is validated using different set experiments and found in close agreement.

1. Introduction

Transmission of signals between a transmitter and a receiver in a communication system encounters different types of dispersive channels. Such channels perform certain non-ideal transformations resulting in different types of interferences like inter-symbol interference (ISI) and frequency selective fading, which are considered to be the biggest limiting factors in a communication system. One of the approaches to combat ISI is to use blind equalizer. An adaptive blind equalizer attempts to compensate for the distortions of the channel by processing the received signals and reconstructing the transmitted signal up to some indeterminacies by the use of linear or nonlinear filters. Specifically, a blind equalizer does not require any training mode and tries to mitigate the effects of the channel solely on the basis of probabilistic and statistical properties of the transmitted data sequence. The basic idea behind an adaptive blind equalizer is to minimize or maximize some admissible blind objective or cost function through the choice of filter coefficients based on the equalizer output [1–3].

When an adaptive equalizer is used to combat a time-varying channel, the optimum Wiener solution takes time-varying form which results in variation of saddle

* Corresponding author. Tel./fax: +92 336 232 1845.
E-mail addresses: ali-waqar.azim@ensimag.grenoble-inp.fr (A.W. Azim), sabrar@comsats.edu.pk (S. Abrar), azzedine@kfupm.edu.sa (A. Zerguine), asoke.nandi@brunel.ac.uk (A.K. Nandi).

http://dx.doi.org/10.1016/j.sigpro.2014.10.020
0165-1684/

point in error performance surface. If the underlying signal statistics happen to change with time, then these statistical variations will be reflected in the data, the filter has access to, which in turn will be reflected in the performance of filters. So, tracking variations in signal statistics or signal moments is considered to be a useful property for adaptive filters. For adaptive filters, the variation in underlying signal statistics and the saddle point can be tracked by using *tracking performance analysis*; and consequently, the filter parameters can be adjusted accordingly to maintain the saddle points of error performance surface and to calculate the variations in underlying signal statistics in time-varying systems. One metric to evaluate tracking performance of an adaptive filter is to measure the steady-state excess mean square error (EMSE). EMSE can be defined as the difference between the mean square error (MSE) of the filter in steady-state and the minimum cost. The smaller the EMSE of an adaptive filter, the better it is [4]. If filter parameters (like step-size) are chosen correctly, the filter can track variations in signal statistics provided variations are not fast. However, tracking fast variations in signal statistics might be a challenging task or at times impossible to perform [4].

In the context of adaptive blind equalization, the widely adopted algorithm is Constant Modulus Algorithm (CMA2-2) [2,5–7]. For quadrature amplitude modulation (QAM) signaling, however, a tailored version of CMA2-2, commonly known as Multimodulus Algorithm (MMA2-2), is considered to be more suitable. The MMA2-2 is capable of jointly achieving blind equalization and carrier phase recovery [8–13], whereas the CMA2-2 requires a separate phase-lock loop for carrier phase recovery.

The nonlinearity of most of the adaptive equalizers, including both CMA2-2 and MMA2-2, makes the steady-state analysis and tracking performance a difficult task to perform. As a result, only a small number of analyses are available in the literature concerning the steady-state analysis performance of adaptive equalizers. However, a few results are available on EMSE analysis of CMA2-2, where some researchers employed Lyapunov stability and averaging analysis [14], and some exploited the variance relation theorem [15,16] to evaluate the same. The steady-state analysis of adaptive filters has gained interest due to ease in analysis owing to variance relation theorem. Abrar et al. [17] performed the EMSE analysis of CMA2-2 and βCMA [18] by assuming that the modulus of equalized signals is Rician distributed in the steady-state. Moreover, this theorem has been employed to study the steady-state analysis of a number of adaptive blind equalization algorithms like in the analyses of the so-called hybrid algorithm [19], the square contour algorithm [20], the improved square contour algorithm [21] and the varying-modulus algorithms [22].

In this paper, we perform tracking performance analysis of two well-known multimodulus equalizers. In particular, using the variance relation arguments, we derive expressions for steady-state EMSE of MMA2-2 and recently proposed βMMA [23] under the assumption that the quadrature components of the successfully equalized signal are Gaussian distributed when conditioned on true signal alphabets. The paper is organized as follows: Section 2 introduces the mathematical model for the system. Section 3 introduces the non-stationary environment and the framework for EMSE analyses. Section 3.1 provides the steady-state tracking performance analysis for MMA2-2 equalizer. Section 3.2 presents the analytical expression evaluated for steady-state tracking performance analysis for βMMA equalizer. Section 4 provides simulation results for steady-state performances of MMA2-2 and βMMA for equalized zero-forcing scenario, equalization of fixed and time-varying channels, and equalization under different values of filter-length. Finally, Section 5 draws conclusions.

2. System model and multimodulus equalizers

A typical baseband communication system is given in Fig. 1. Consider the transmission of discrete valued complex sequence $\{a_n\}$ over an unknown communication channel characterized by finite impulse response filter with impulse response $\boldsymbol{h}_n$; the sequence $\{a_n\}$ is independent and identically distributed (i.i.d.), and takes value of square-QAM symbols with equal probability. The considered channel $\boldsymbol{h}_n$ is a fading, dispersive, time-varying in nature, where the channel at index n is given as $\boldsymbol{h}_n = \boldsymbol{h}_{\text{const}} + \boldsymbol{c}_n$. The channel is a complex Gaussian random process with a constant mean $\boldsymbol{h}_{\text{const}}$ (because of shadowing, reflections and large scale path loss) and a time-variant part $\boldsymbol{c}_n$, the channel taps vary from symbol to symbol and are modeled as mutually uncorrelated circular complex Gaussian random processes. The time-varying part of the channel can be modeled by a pth-order autoregressive process AR(p).

The received signal x_n is the convolution of transmitted sequence $\{a_n\}$ and filter impulse response $\boldsymbol{h}_n$ represented as $x_n = \boldsymbol{h}_n^T \boldsymbol{a}_n$, where superscript T denotes the transpose operator. The vector $\boldsymbol{x}_n$ is fed to the equalizer to combat the interference introduced by the physical channel and estimate delayed version of the transmitted sequence $\{a_{n-\delta}\}$, where δ denotes delay.

Let $\boldsymbol{w}_n = \left[w_{n,0}, w_{n,1}, \ldots, w_{n,N-1}\right]^T$ be the impulse response of equalizer and $\boldsymbol{x}_n = \left[x_n, x_{n-1}, \ldots, x_{n-N+1}\right]^T$ be the regression vector (vector of channel observations), N is the number of equalizer taps. The output of equalizer is convolution of regression vector and equalizer impulse response given as $y_n = \boldsymbol{w}_{n-1}^H \boldsymbol{x}_n$ where superscript H denotes the Hermitian conjugate operator. Let $\boldsymbol{t}_n = \boldsymbol{h}_n \otimes \boldsymbol{w}_{n-1}^*$ be the overall channel-equalizer impulse response ($\otimes$ denotes convolution operation and the superscript $*$ denotes complex conjugate operator). If the channel response is given by a K-tap vector $\boldsymbol{h}_n = [h_{n,0}, h_{n,1}, \ldots,$

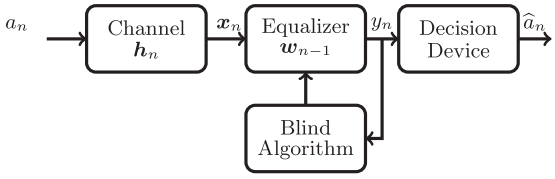

Fig. 1. A typical baseband communication system.

$h_{n,K-1}]$, then the channel convolution matrix $\mathcal{H}$ is given by

$$\mathcal{H}=\begin{bmatrix} h_{n,0} & 0 & \cdots & 0 & \cdots \\ h_{n,1} & h_{n,0} & \ddots & 0 & \ddots \\ \vdots & h_{n,1} & \ddots & \vdots & \ddots \\ h_{n,K-1} & \vdots & \ddots & h_{n,0} & \ddots \\ 0 & h_{n,K-1} & \ddots & h_{n,1} & \ddots \\ \vdots & \vdots & \cdots & \ddots & \ddots \end{bmatrix} \tag{1}$$

Using (1), we obtain $\boldsymbol{t}_n=\boldsymbol{h}_n\otimes\boldsymbol{w}_{n-1}^*=\mathcal{H}\boldsymbol{w}_{n-1}^*$. Under successful convergence, we have $\boldsymbol{t}_n=\boldsymbol{e}$ where $\boldsymbol{e}=[0,\ldots,0,1,0,\ldots,0]^T$.

Consider a generic stochastic gradient-based adaptive equalizer [4] for which the updating algorithm is given as

$$\boldsymbol{w}_n=\boldsymbol{w}_{n-1}+\mu\Phi(y_n)^*\boldsymbol{x}_n \tag{2}$$

where μ is a small positive step size, governing the speed of convergence and the level of steady-state equalizer performance, and $\Phi(y_n)$ is complex valued *error-function*. In principle, $\Phi(y_n)$ satisfies the Bussgang condition on successful convergence [24], *i.e.*, $\mathrm{E}[y_n\Phi(y_{n-i})^*]=0,\forall i,n$. The error-function of a multimodulus equalizer is non-analytic in nature, *i.e.*, it is a decoupled function of the quadrature components of deconvolved sequence y_n, which is expressed as

$$\Phi(y_n)=\phi(y_{R,n})+j\phi(y_{I,n}), \tag{3}$$

so that the real and imaginary parts of $\Phi(y_n)$ are obtained from the real and imaginary parts of y_n, $y_{R,n}$ and $y_{I,n}$, respectively.

2.1. The MMA2-2 equalizer

The MMA2-2 equalization algorithm was proposed independently in [9,10,25], which employs a split cost function

$$J^{\mathrm{MMA2-2}}=\min_{\boldsymbol{w}}\left\{\mathrm{E}\left(y_{R,n}^2-R_R^2\right)^2+\mathrm{E}\left(y_{I,n}^2-R_I^2\right)^2\right\} \tag{4}$$

where R_R and R_I are defined as $R_R^2:=\mathrm{E}a_R^4/\mathrm{E}a_R^2$ and $R_I^2:=\mathrm{E}a_I^4/\mathrm{E}a_I^2$, in which a_R and a_I denote the real and imaginary parts of transmitted sequence $\{a_n\}$, respectively. The MMA2-2 cost function can be considered as the sum of two one-dimensional cost functions, expressing the dispersion of the equalizer in the complex constellation plane. The tap weight vector of MMA2-2 is updated according to

$$\boldsymbol{w}_n=\boldsymbol{w}_{n-1}+\mu\left[(R_R^2-y_{R,n}^2)y_{R,n}+j(R_I^2-y_{I,n}^2)y_{I,n}\right]^*\boldsymbol{x}_n \tag{5}$$

Notably, due to its decoupled error-function, MMA2-2 is capable of compensating residual phase-offset and moderate frequency-offset mismatches without requiring additional hardware. Interested readers may refer to [26,27] for discussions on phase recovery capability of MMA2-2. As far as ISI cancellation capability is concerned, the stationary points of MMA2-2 are closely related to those of CMA2-2 [8,11]. For the sake of comparison, the CMA2-2 update is $\boldsymbol{w}_n=\boldsymbol{w}_{n-1}+\mu(R^2-|y_n|^2)y_n^*\boldsymbol{x}_n$.

2.2. The βMMA equalizer

Recently, Abrar and Nandi [23] have proposed a new multimodulus algorithm, the βMMA, for joint blind equalization and carrier phase recovery in square-QAM signaling. The algorithm is derived by solving a constrained maximization problem. Results have indicated a superior performance to be exhibited by βMMA, for higher-order QAM signaling on both symbol and fractionally spaced channels, as compared to established methods including MMA2-2 and CMA2-2. The cost function of βMMA is given as [23].[1]

$$J^{\beta\mathrm{MMA}}=\max_{\boldsymbol{w}}\left\{\mathrm{E}y_{R,n}^2+\mathrm{E}y_{I,n}^2\right\}\quad\text{subject to }\max\{|y_{R,n}|\}=\max\{|y_{I,n}|\}\le\gamma \tag{6}$$

where γ is the largest amplitude of quadrature component; for M-ary square-QAM with signal levels $\{\pm1,\pm3,\ldots,\pm\gamma\}$, we have $\gamma=\sqrt{M}-1$. The tap weight vector of βMMA is updated according to

$$\boldsymbol{w}_n=\boldsymbol{w}_{n-1}+\mu\left(f_R y_{R,n}+jf_I y_{I,n}\right)^*\boldsymbol{x}_n \tag{7}$$

where f_L is equal to unity if $|y_{L,n}|\le\gamma$, and it is equal to $-\beta$, otherwise (where L denotes either R or I). The parameter β is a statistical constant whose value is evaluated to be equal to $(\gamma^2+2)/(3\gamma)$.

3. Non-stationary environment and EMSE analysis

In order to perform tracking analysis, we consider a non-stationary system model. In such environment, the variations in the Wiener solution (zero-forcing solution or optimal equalizer), $\boldsymbol{w}^o$, follow (usually) first-order random walk model [4]. The optimal weights from one iteration to another are described by

$$\boldsymbol{w}_n^o=\boldsymbol{w}_{n-1}^o+\boldsymbol{q}_n \tag{8}$$

where the new weight is the previous weight plus a random fluctuation denoted by $\boldsymbol{q}_n$. The random vector $\boldsymbol{q}_n$ is independent and identically distributed (i.i.d.) zero-mean random vector whose positive definite covariance matrix is given as $\boldsymbol{Q}=\mathrm{E}\boldsymbol{q}_n\boldsymbol{q}_n^H=\sigma_q^2\boldsymbol{I}$, where σ_q is the standard deviation of $\boldsymbol{q}_n$ (E denotes expected value). We are going to assume that $\boldsymbol{q}_n$ is independent of both $\{a_m\}$ and $\{\boldsymbol{x}_m,\boldsymbol{w}_{-1}^o\}$ for all $m<n$ [4]. Using the Wiener solution, the desired data a_n can be expressed as

$$a_n=(\boldsymbol{w}_{n-1}^o)^H\boldsymbol{x}_n+v_n, \tag{9}$$

where v_n is the measurement noise and is uncorrelated with $\boldsymbol{x}_n$, $\mathrm{E}(v_n^*\boldsymbol{x}_n)=0$ [29]. Defining weight error vector $\tilde{\boldsymbol{w}}_n$ as $\tilde{\boldsymbol{w}}_n:=\boldsymbol{w}_n^o-\boldsymbol{w}_n$, (2) for non-stationary case can be rewritten as

$$\tilde{\boldsymbol{w}}_n=\tilde{\boldsymbol{w}}_{n-1}-\mu\Phi(y_n)^*\boldsymbol{x}_n+\boldsymbol{q}_n \tag{10}$$

The so-called *a priori* and *a posteriori* estimation errors are defined as $e_{a,n}:=\tilde{\boldsymbol{w}}_{n-1}^H\boldsymbol{x}_n$ and $e_{p,n}:=(\tilde{\boldsymbol{w}}_n-\boldsymbol{q}_n)^H\boldsymbol{x}_n$,

[1] The cost (6) first appeared in [28] and was solved by quadratic programming.

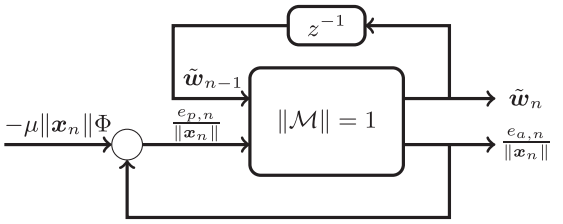

Fig. 2. Lossless mapping and feedback loop.

respectively. After some mathematical manipulations, one gets [4]

$$e_{a,n} = e_{p,n} + \mu\|\boldsymbol{x}_n\|^2 \Phi(y_n) \tag{11}$$

where $\|\cdot\|$ represents the Euclidean norm. It is important to note that $e_{a,n}$ depends on channel variation, adaption, and gradient noise. The steady-state EMSE and tracking performance of an adaptive equalizer can be quantified by the energy of $e_{a,n}$. From (11), we can associate the error-function of an equalizer with the *a priori* and the *a posteriori* estimation errors as follows:

$$\Phi(y_n) = \frac{e_{a,n} - e_{p,n}}{\mu\|\boldsymbol{x}_n\|^2} \tag{12}$$

Substituting (12) in (10), and after some mathematical manipulation we obtain the energy conservation relation as follows:

$$\|\tilde{\boldsymbol{w}}_n\|^2 + \frac{|e_{a,n}|^2}{\|\boldsymbol{x}_n\|^2} = \|\tilde{\boldsymbol{w}}_{n-1}\|^2 + \frac{|e_{p,n}|^2}{\|\boldsymbol{x}_n\|^2} \tag{13}$$

It is important to note that (13) holds for any adaptive algorithm. Fig. 2 represents the physical interpretation of (13), which links the energies of the weight error vector, the *a priori* and the *a posteriori* estimation errors by stating that mapping from the variables $\{\tilde{\boldsymbol{w}}_{n-1}, e_{p,n}/\|\boldsymbol{x}_n\|\}$ to the variables $\{\tilde{\boldsymbol{w}}_n, e_{a,n}/\|\boldsymbol{x}_n\|\}$ is energy preserving. The function $\mathcal{M}$ denotes the mapping between the two variables and z^{-1} denotes the unit delay operator.

Substituting the value of $e_{p,n}$ from (11) into (13), we get the following (variance relation) theorem:

Theorem 1 (Variance Relation, *Sayed [4]*). *Consider any adaptive filter of the form (2), and assume filter operation in steady-state. Assume further that* $a_n = (\boldsymbol{w}^o_{n-1})^H \boldsymbol{x}_n + v_n$, *where* $\boldsymbol{w}^o_{n-1}$ *varies according to the random-walk model (8), where* $\boldsymbol{q}_n$ *is a zero-mean i.i.d. sequence with covariance matrix* $\boldsymbol{Q}$. *Moreover,* $\boldsymbol{q}_n$ *is independent of* $\{a_m\}$ *and* $\{\boldsymbol{x}_m, \boldsymbol{w}^o_{-1}\}$ *for all* $m < n$. *Having* $y_n = a_n - e_{a,n}$, *it holds that*

$$2\mathrm{E}\Re\left[e^*_{a,n}\Phi(y_n)\right] = \mu\mathrm{E}\|\boldsymbol{x}_n\|^2\mathrm{E}|\Phi(y_n)|^2 + \mu^{-1}\mathrm{E}\|\boldsymbol{q}_n\|^2 \tag{T1.1}$$

where $\Re[\cdot]$ *denotes the real part of complex entity.*

Expression (T1.1) can be solved for steady-state EMSE, which is defined as

$$\mathrm{EMSE} \triangleq \lim_{n\to\infty} \mathrm{E}|e_{a,n}|^2 \tag{14}$$

The procedure of evaluating EMSE using (T1.1) avoids the need of explicit evaluation of $\mathrm{E}\|\tilde{\boldsymbol{w}}_n\|^2$ or its steady-state value $\mathrm{E}\|\tilde{\boldsymbol{w}}_\infty\|^2$. In the sequel, in addition to variance relation, we aim to make use of the following assumptions:

(A1) In steady-state the *a priori* error $e_{a,n}$ is independent of both the transmitted sequence $\{a_n\}$ and the regressor vector $\boldsymbol{x}_n$ [4].

(A2) The filter taps are large enough so that by virtue of central limit theorem, $e_{a,n}$ is the zero-mean complex valued Gaussian [29,30].

(A3) The optimum filter achieves perfect equalization (zero-forcing solution) $a_n \approx (\boldsymbol{w}^o_{n-1})^H \boldsymbol{x}_n$, however due to channel variation and gradient noise, the equalizer weight vector is not equal to $\boldsymbol{w}^o_n$ even in steady-state [31]. Additionally, no additive noise is assumed in the system.

Assumption (**A1**) is the orthogonality condition required for a successful convergence. The assumption (**A2**) about the Gaussianity of *a priori* estimation error has appeared in a number of recent researches. For example, Bellini [24] discussed that the convolutional noise (which bears similar mathematical definition as that of *a priori* estimation error) may be considered as zero-mean Gaussian, and same is the opinion of Vaseghi [32]. Moreover, Ref. [33] discussed that the *a priori* estimation error (for a long equalizer) may be modeled as zero-mean Gaussian random variable. It has been shown that the steady-state *a priori* estimation error is zero-mean Gaussian even for the case where the measurement noise is taken to be uniformly distributed. The assumption (**A3**) is based on the understanding that CMA2-2 and similarly its multimodulus variants diverge on infinite time horizon when noise is unbounded. Interested readers may refer to [34] for a detailed discussion on this issue. Note that the (total) mean square error, MSE of a non-diverging equalizer in the presence of additive noise, however, can always be given as $\mathrm{MSE} = \sigma_v^2 + \mathrm{EMSE}$, where σ_v^2 is the variance of modeling error/measurement noise.

Here onwards, for the sake of notational simplicity, we employ $\zeta := \mathrm{EMSE}$, $e_a := e_{a,n}$, $y := y_n$, $a := a_n$, $\Phi := \Phi(y_n)$, $P_x = \mathrm{E}\|\boldsymbol{x}_n\|^2$, $P_q = \mathrm{E}\|\boldsymbol{q}_n\|^2$ and $P_a = \mathrm{E}|a|^2 = \mathrm{E}(a_R^2 + a_I^2)$.

3.1. The EMSE of MMA2-2 equalizer

In order to evaluate the analytical expression for the steady-state EMSE of MMA2-2, we need to evaluate the energy of error-function as well as its correlation with *a priori* estimation error. Implementing these steps, we have the following theorem for the tracking performance of MMA2-2 equalizer:

Theorem 2 (Tracking EMSE of MMA2-2). *Consider the* MMA2-2 *recursion (5) with complex-valued data. Considering non-stationary model (8) with a sufficiently small degree of non-stationarity. Then its EMSE can be approximated by the following expression for a sufficiently small step-size* μ:

$$\zeta^{\mathrm{MMA2-2}}(\mu) = \frac{\mu c_1 + \frac{1}{\mu} P_q}{c_2 - \mu c_3}, \tag{T2.1}$$

$$\mu_{\text{opt}}^{\text{MMA2-2}} = \frac{\sqrt{P_q c_1 c_2^2 + P_q^2 c_3^2} - P_q c_3}{c_1 c_2} \quad \textit{with } \zeta_{\min}^{\text{MMA2-2}} = \frac{2P_q}{\mu_{\text{opt}} c_2} \tag{T2.2}$$

where $c_1 := 2P_x(\text{E}a_R^6 - 2R_R^2\text{E}a_R^4 + R_R^4\text{E}a_R^2)$, $c_2 := 2(3\text{E}a_R^2 - R_R^2)$, *and* $c_3 := P_x(3\text{E}a_R^4 + R_R^4)$. *Substituting the expression for* μ_{opt} *into the expression of EMSE we find the corresponding optimal EMSE.*

Proof. The error-function of MMA2-2 equalizer is given by $\Phi = (R_R^2 - y_R^2)y_R + j(R_I^2 - y_I^2)y_I$. Towards evaluating the RHS of (T1.1), we compute $\text{E}|\Phi|^2$ as follows:

$$\text{E}|\Phi|^2 = R_R^4\text{E}y_R^2 - 2R_R^2\text{E}y_R^4 + \text{E}y_R^6 + R_I^4\text{E}y_I^2 - 2R_I^2\text{E}y_I^4 + \text{E}y_I^6 \tag{15}$$

For the given value of a, owing to (**A2**), the quadrature components of the equalizer output y may be modeled as Gaussian distributed so that its density is given by

$$\text{p}(y_L|a_L) = \frac{1}{\sqrt{2\pi}\sigma}\exp\left(-\frac{(y_L - a_L)^2}{2\sigma^2}\right) \tag{16}$$

where $\sigma^2 := \text{E}\Re[e_a]^2 = \text{E}\Im[e_a]^2$, *i.e.*, $\zeta = 2\sigma^2$. Using (16), the required moments in (15) may be computed as $\text{E}y_L^p = \int_{-\infty}^{\infty} y_L^p \text{p}(y_L|a_L)\,\text{d}y_L$, which gives $\text{E}y_L^2 = \text{E}a_L^2 + \frac{\zeta}{2}$, $\text{E}y_L^4 = \text{E}a_L^4 + 3\zeta\text{E}a_L^2 + \frac{3}{4}\zeta^2$, and $\text{E}y_L^6 = \text{E}a_L^6 + \frac{15}{2}\zeta\text{E}a_L^4 + \frac{45}{4}\zeta^2\text{E}a_L^2 + \frac{15}{8}\zeta^3$. Substituting the computed moments in (15), we obtain

$$\begin{aligned}\text{E}|\Phi|^2 = {} & \tfrac{30}{8}\zeta^3 + \zeta^2\left(\tfrac{45}{4}\text{E}a_R^2 - \tfrac{3}{2}R_R^2 + \tfrac{45}{4}\text{E}a_I^2 - \tfrac{3}{2}R_I^2\right) \\ & + \zeta\left(\tfrac{3}{2}\text{E}a_R^4 + \tfrac{1}{2}R_R^4 + \tfrac{3}{2}\text{E}a_I^4 + \tfrac{1}{2}R_I^4\right) + \text{E}a_R^6 \\ & + R_R^4\text{E}a_R^2 - 2R_R^2\text{E}a_R^4 + \text{E}a_I^6 + R_I^4\text{E}a_I^2 - 2R_I^2\text{E}a_I^4\end{aligned} \tag{17}$$

Thus, the RHS of (T1.1) is computed as

$$\begin{aligned}\text{RHS} = {} & \mu P_x\left(\tfrac{30}{8}\zeta^3 + \zeta^2\left(\tfrac{45}{4}\text{E}a_R^2 - \tfrac{3}{2}R_R^2 + \tfrac{45}{4}\text{E}a_I^2 - \tfrac{3}{2}R_I^2\right)\right. \\ & + \zeta\left(\tfrac{3}{2}\text{E}a_R^4 + \tfrac{1}{2}R_R^4 + \tfrac{3}{2}\text{E}a_I^4 + \tfrac{1}{2}R_I^4\right) + \text{E}a_R^6 + R_R^4\text{E}a_R^2 \\ & \left. - 2R_R^2\text{E}a_R^4 + \text{E}a_I^6 + R_I^4\text{E}a_I^2 - 2R_I^2\text{E}a_I^4\right) + \mu^{-1}P_q\end{aligned} \tag{18}$$

Since $e_a^* = (a_R - y_R) - j(a_I - y_I)$. Substituting e_a^* in (T1.1), the LHS is evaluated as $\text{LHS} = 2\text{E}\Re[e_a^*\Phi] = 2R_R^2\text{E}a_R y_R - 2\text{E}a_R y_R^3 - 2R_R^2\text{E}y_R^2 + 2\text{E}y_R^4 + 2R_I^2\text{E}a_I y_I - 2\text{E}a_I y_I^3 - 2R_I^2\text{E}y_I^2 + 2\text{E}y_I^4$. Substituting $y_L = (a_L - e_{aL})$ and evaluating the expectation, we get $\text{E}a_L y_L = \text{E}a_L^2$ and $\text{E}a_L y_L^3 = (\text{E}a_L^4 + \frac{3}{2}\zeta\text{E}a_L^2)$. Finally, we get

$$\text{LHS} = 3\zeta^2 + \zeta(3\text{E}a_R^2 - R_R^2 + 3\text{E}a_I^2 - R_I^2) \tag{19}$$

Combining (18) and (19), we obtain

$$\begin{aligned}& \tfrac{30}{8}\zeta^3\mu P_x + \zeta^2\left(\mu P_x\left(\tfrac{45}{4}\text{E}a_R^2 - \tfrac{3}{2}R_R^2 + \tfrac{45}{4}\text{E}a_I^2 - \tfrac{3}{2}R_I^2\right) - 3\right) \\ & + \zeta\left(\mu P_x\left(\tfrac{3}{2}\text{E}a_R^4 + \tfrac{1}{2}R_R^4 + \tfrac{3}{2}\text{E}a_I^4 + \tfrac{1}{2}R_I^4\right)\right. \\ & \left. - 3\text{E}a_R^2 + R_R^2 - 3\text{E}a_I^2 + R_I^2\right) \\ & + \mu P_x\left(\text{E}a_R^6 + R_R^4\text{E}a_R^2 - 2R_R^2\text{E}a_R^4 + \text{E}a_I^6 + R_I^4\text{E}a_I^2 - 2R_I^2\text{E}a_I^4\right) \\ & + \mu^{-1}P_q = 0\end{aligned} \tag{20}$$

The QAM constellation exhibits four-quadrant symmetry which implies $\text{E}a_R^p = \text{E}a_I^p$ and $R_R = R_I$. So, Eq. (20) can be rewritten just in terms of real components and this yields a cubic expression to solve for EMSE of MMA2-2 equalizer as given by

$$\begin{aligned}& \tfrac{30}{8}\zeta^3\mu P_x + \zeta^2\left(\mu P_x\left(\tfrac{90}{4}\text{E}a_R^2 - 3R_R^2\right) - 3\right) \\ & - \zeta\left(6\text{E}a_R^2 - 2R_R^2 - \mu P_x\left(3\text{E}a_R^4 + R_R^4\right)\right) \\ & + \mu P_x\left(2\text{E}a_R^6 + 2R_R^4\text{E}a_R^2 - 4R_R^2\text{E}a_R^4\right) + \mu^{-1}P_q = 0\end{aligned} \tag{21}$$

[2]In order to evaluate some closed-form expressions of $\zeta^{\text{MMA2-2}}$, certain approximations have to be made, *e.g.*, by neglecting the cubic and quadratic terms in (21), we obtain

$$\begin{aligned}& \zeta(\mu P_x(3\text{E}a_R^4 + R_R^4) - 6\text{E}a_R^2 + 2R_R^2) + \mu P_x(2\text{E}a_R^6 + 2R_R^4\text{E}a_R^2 \\ & - 4R_R^2\text{E}a_R^4) + \mu^{-1}P_q = 0\end{aligned} \tag{22}$$

which yields the following closed-form solution:

$$\zeta^{\text{MMA2-2}} = \frac{\mu^2 P_x\left(2\text{E}a_R^6 + 2R_R^4\text{E}a_R^2 - 4R_R^2\text{E}a_R^4\right) + P_q}{\mu(6\text{E}a_R^2 - 2R_R^2) - \mu^2 P_x(3\text{E}a_R^4 + R_R^4)} \tag{23}$$

Using (23) and solving $\nabla_\mu \zeta^{\text{MMA2-2}} = 0$, the optimum μ is obtained as

$$\mu_{\text{opt}}^{\text{MMA2-2}} = \frac{\sqrt{P_q c_1 c_2^2 + P_q^2 c_3^2} - P_q c_3}{c_1 c_2} \tag{24}$$

where $c_1 := P_x(2\text{E}a_R^6 + 2R_R^4\text{E}a_R^2 - 4R_R^2\text{E}a_R^4)$, $c_2 := 6\text{E}a_R^2 - 2R_R^2$, and $c_3 := P_x(3\text{E}a_R^4 + R_R^4)$. Expression (24) leads to the minimum EMSE, $\zeta_{\min}^{\text{MMA2-2}}$, as follows:

$$\zeta_{\min}^{\text{MMA2-2}} = \frac{P_q}{\mu_{\text{opt}}(3\text{E}a_R^2 - R_R^2)} \tag{25}$$

which completes the proof. □

Since $R_R^2 = \text{E}a_R^4/\text{E}a_R^2$, we express $\zeta_{\min}^{\text{MMA2-2}} = P_q\text{E}a_R^2/\left(\mu_{\text{opt}}(3(\text{E}a_R^2)^2 - \text{E}a_R^4)\right)$. Note that the quantity, $\kappa_{a_R} := \text{E}a_R^4 - 3(\text{E}a_R^2)^2$, is the kurtosis of the quadrature component of transmitted signal a_n and it is a negative quantity due to the sub-Gaussian nature of a_n. Denoting $\sigma_{a_R}^2 := \text{E}a_R^2$, we obtain

$$\zeta_{\min}^{\text{MMA2-2}} = \frac{P_q\sigma_{a_R}^2}{\mu_{\text{opt}}|\kappa_{a_R}|} \tag{26}$$

Expression (26) implies that if the transmitted signal tends to be Gaussian (*i.e.*, $\kappa_{a_R} \to 0$), then the equalizer implementing MMA2-2 will diverge without bound. This behavior is in accordance with the Benveniste–Goursat–Ruget theorem [35], which states that the transmitted signal is required necessarily to be non-Gaussian in order to get equalized.

[2] Here, we emphasize that no approximations were involved in the derivation of (21). Also, it is experimentally observed that EMSE is the smallest positive root of (21).

3.2. The EMSE of βMMA equalizer

Under similar conditions and assumptions, as mentioned in Section 3.1, we have the following theorem for tracking performance of βMMA:

Theorem 3 (Tracking EMSE of βMMA). *Consider the βMMA recursion (7) with complex-valued data. Considering the non-stationary model (8) with a sufficiently small degree of non-stationarity, its* EMSE *can be approximated by the following expression for a sufficiently small step-size* μ:

$$\zeta^{\beta\text{MMA}}(\mu)=\left(\frac{c_4+c_3\mu+\sqrt{(c_4+c_3\mu)^2-4(c_2+c_1\mu)\left(c_5\mu+\frac{1}{\mu}P_q\right)}}{2(c_2+c_1\mu)}\right)^2, \tag{T3.1}$$

$$\mu_{\text{opt}}^{\beta\text{MMA}}=\sqrt{\frac{P_q}{c_5}}\quad \textit{with}\ \zeta_{\min}^{\beta\text{MMA}}=\zeta^{\beta\text{MMA}}\left(\mu_{\text{opt}}^{\beta\text{MMA}}\right), \tag{T3.2}$$

where $c_1:=P_x(1+(1/\sqrt{M})(\beta^2-1))$, $c_2:=2(1-(1/\sqrt{M})(\beta+1))$, $c_3:=(2/\sqrt{\pi M})\gamma P_x(\beta^2-1)$, $c_4:=-(4/\sqrt{\pi M})\gamma(\beta+1)$, *and* $c_5:=(P_a+(2/\sqrt{M})\gamma^2(\beta^2-1))P_x$. *Substituting the expression for* μ_{opt} *into the expression of EMSE we find the corresponding optimal EMSE.*

Proof. The error-function of βMMA equalizer is given as $\Phi=f_R y_R+jf_I y_I$. The RHS of (T1.1) for βMMA is thus evaluated as follows:

$$\begin{aligned}\mathrm{E}|\Phi|^2&=\mathrm{E}\left[y_{R\{|y_R|<\gamma\}}^2+\beta^2 y_{R\{|y_R|>\gamma\}}^2+y_{I\{|y_I|<\gamma\}}^2+\beta^2 y_{I\{|y_I|>\gamma\}}^2\right]\\&=\mathrm{E}y_R^2+2(\beta^2-1)\mathrm{E}y_{R_{\{y_R>\gamma\}}}^2+\mathrm{E}y_I^2+2(\beta^2-1)\mathrm{E}y_{I_{\{y_I>\gamma\}}}^2\\&=\mathrm{E}a_R^2+\zeta+2(\beta^2-1)\\&\quad\times\mathrm{E}\left[\frac{1}{\sqrt{2\pi}}\exp\left(-\frac{(a_R-\gamma)^2}{\zeta}\right)(a_R+\gamma)\sqrt{\frac{\zeta}{2}}\right.\\&\quad\left.+\frac{1}{2}\left(a_R^2+\frac{\zeta}{2}\right)\left(1+\mathrm{erf}\left(\frac{a_R-\gamma}{\sqrt{\zeta}}\right)\right)\right]\\&\quad+\mathrm{E}a_I^2+2(\beta^2-1)\mathrm{E}\left[\frac{1}{\sqrt{2\pi}}\exp\left(-\frac{(a_I-\gamma)^2}{\zeta}\right)(a_I+\gamma)\sqrt{\frac{\zeta}{2}}\right.\\&\quad\left.+\frac{1}{2}\left(a_I^2+\frac{\zeta}{2}\right)\left(1+\mathrm{erf}\left(\frac{a_I-\gamma}{\sqrt{\zeta}}\right)\right)\right]\end{aligned} \tag{27}$$

where erf(·), the *Gauss error function*, is defined as $\mathrm{erf}(x)=(2/\sqrt{\pi})\int_0^x\exp(-t^2)\,\mathrm{d}t$. Using (27), the RHS of (T1.1) for βMMA equalizer becomes

$$\begin{aligned}\mathrm{RHS}&=\mu P_x\left[\mathrm{E}a_R^2+\zeta+2(\beta^2-1)\right.\\&\quad\times\mathrm{E}\left[\frac{1}{\sqrt{2\pi}}\exp\left(-\frac{(a_R-\gamma)^2}{\zeta}\right)(a_R+\gamma)\sqrt{\frac{\zeta}{2}}\right.\\&\quad\left.+\frac{1}{2}\left(a_R^2+\frac{\zeta}{2}\right)\left(1+\mathrm{erf}\left(\frac{a_R-\gamma}{\sqrt{\zeta}}\right)\right)\right]+\mathrm{E}a_I^2\\&\quad+2(\beta^2-1)\mathrm{E}\left[\frac{1}{\sqrt{2\pi}}\exp\left(-\frac{(a_I-\gamma)^2}{\zeta}\right)(a_I+\gamma)\sqrt{\frac{\zeta}{2}}\right.\\&\quad\left.\left.+\frac{1}{2}\left(a_I^2+\frac{\zeta}{2}\right)\left(1+\mathrm{erf}\left(\frac{a_I-\gamma}{\sqrt{\zeta}}\right)\right)\right]\right]+\mu^{-1}P_q\end{aligned} \tag{28}$$

Next substituting the *a priori* error in (T1.1), the LHS for βMMA is evaluated as

$$\begin{aligned}\mathrm{LHS}&=2\mathrm{E}\Re\left[e_a^*\Phi\right]=2\mathrm{E}\left[a_R f_R y_R-f_R y_R^2+a_I f_I y_I-f_I y_I^2\right]\\&=2\mathrm{E}(a_R y_R-y_R^2)-4(\beta+1)\mathrm{E}(a_R y_R-y_R^2)_{\{y_R>\gamma\}}\\&\quad+2\mathrm{E}(a_I y_I-y_I^2)-4(\beta+1)\mathrm{E}(a_I y_I-y_I^2)_{\{y_I>\gamma\}}\end{aligned} \tag{29}$$

Exploiting assumption (**A2**), we obtain

$$\begin{aligned}\mathrm{LHS}&=-2\zeta+4(\beta+1)\mathrm{E}\left[\frac{\gamma}{2}\sqrt{\frac{\zeta}{\pi}}\exp\left(-\frac{(a_R-\gamma)^2}{\zeta}\right)+\frac{\zeta}{4}\left(1+\mathrm{erf}\left(\frac{a_R-\gamma}{\sqrt{\zeta}}\right)\right)\right]\\&\quad+4(\beta+1)\mathrm{E}\left[\frac{\gamma}{2}\sqrt{\frac{\zeta}{\pi}}\exp\left(-\frac{(a_L-\gamma)^2}{\zeta}\right)+\frac{\zeta}{4}\left(1+\mathrm{erf}\left(\frac{a_L-\gamma}{\sqrt{\zeta}}\right)\right)\right]\end{aligned} \tag{30}$$

Owing to four quadrant symmetry of QAM constellation, the moments evaluated for in-phase component are same as those for quadrature component. Simplifying and combining (28) and (30), we obtain

$$\mu P_x(2\mathrm{E}a_R^2+\zeta+4(\beta^2-1)A)+\mu^{-1}P_q+2\zeta-8(\beta+1)B=0 \tag{31}$$

where

$$A:=\mathrm{E}\left[\frac{1}{\sqrt{2\pi}}\exp\left(-\frac{(a_R-\gamma)^2}{\zeta}\right)(a_R+\gamma)\sqrt{\frac{\zeta}{2}}+\frac{1}{2}\left(a_R^2+\frac{\zeta}{2}\right)\left(1+\mathrm{erf}\left(\frac{a_R-\gamma}{\sqrt{\zeta}}\right)\right)\right],$$

$$\text{and } B:=\mathrm{E}\left[\frac{\gamma}{2}\sqrt{\frac{\zeta}{\pi}}\exp\left(-\frac{(a_R-\gamma)^2}{\zeta}\right)+\frac{\zeta}{4}\left(1+\mathrm{erf}\left(\frac{a_R-\gamma}{\sqrt{\zeta}}\right)\right)\right].$$

Since the argument inside the exponent function, $(a_R-\gamma)^2$, is always positive, we have $\exp(\cdot)=0$ for $a_R\neq\gamma$ and $\zeta\ll1$. However, when $a_R=\gamma$, we have $\exp(\cdot)=1$ with probability $\mathrm{P}_r[a_R=\gamma]$. Similarly, under the assumption $\zeta\ll1$, erf(·) is equal to -1, and 0, respectively, for the cases $(a_R<\gamma)$, and $(a_R=\gamma)$. These considerations yield

$$A\approx\begin{cases}0 & \text{if } a_R\neq\gamma\\ \left(\gamma\sqrt{\frac{\zeta}{\pi}}+\frac{1}{2}\left(\gamma^2+\frac{1}{2}\zeta\right)\right)\mathrm{P}_r[a_R=\gamma] & \text{if} a_R=\gamma\end{cases} \tag{32}$$

$$\text{and } B\approx\begin{cases}0 & \text{if } a_R\neq\gamma\\ \left(\gamma\sqrt{\frac{\zeta}{2\pi}}+\frac{1}{4}\zeta\right)\mathrm{P}_r[a_R=\gamma] & \text{if } a_R=\gamma\end{cases} \tag{33}$$

Since an M-point constellation is being considered, the probability $\mathrm{P}_r[a_R=\gamma]$ is equal to $1/\sqrt{M}$. Denoting $c_1:=P_x(1+(1/\sqrt{M})(\beta^2-1))$, $c_2:=2(1-(1/\sqrt{M})(\beta+1))$, $c_3:=(2/\sqrt{\pi M})\gamma P_x(\beta^2-1)$, $c_4:=-(4/\sqrt{\pi M})\gamma(\beta+1)$, and $c_5:=(P_a+(2/\sqrt{M})\gamma^2(\beta^2-1))P_x$, and by combining (31)–(33), we obtain

$$(c_2+c_1\mu)\zeta+(c_4+c_3\mu)\sqrt{\zeta}+\left(c_5\mu+\frac{1}{\mu}P_q\right)=0. \tag{34}$$

Solving it by quadratic formula we obtain (T3.1).

Further, substituting $\zeta=u^2$ and taking derivative with respect to μ, we obtain

$$(c_1u+c_3)u+(c_4+c_3\mu+2(c_2+c_1\mu)u)\frac{\mathrm{d}u}{\mathrm{d}\mu}+\left(c_5-\frac{1}{\mu^2}P_q\right)=0 \tag{35}$$

For the optimum value of μ, we have $\mathrm{d}u/\mathrm{d}\mu=0$; this gives

$$\mu_{\text{opt}}^{\beta\text{MMA}}=\sqrt{\frac{P_q}{c_1\zeta_{\min}^{\beta\text{MMA}}+c_3\sqrt{\zeta_{\min}^{\beta\text{MMA}}}+c_5}} \tag{36}$$

Table 1
Optimum EMSE for 16-QAM.

$\zeta_{\min}^{\text{MMA2-2}}$	Numerical (21)	Closed-form (T2.2)	MC simulation
$N=7$	−15.92 dB	−15.89 dB	−16.13 dB
$N=21$	−10.83 dB	−10.77 dB	−10.85 dB
$\zeta_{\min}^{\beta\text{MMA}}$	Numerical (31)	Closed-form (T3.2)	MC Simulation
$N=7$	−27.61 dB	−27.62 dB	−27.55 dB
$N=21$	−17.86 dB	−17.88 dB	−17.87 dB

Since $c_1\zeta_{\min}^{\beta\text{MMA}}+c_3(\zeta_{\min}^{\beta\text{MMA}})^{0.5}\ll c_5$, ignoring them we obtain (T3.2). □

4. Simulation results

In this section, we verify the tracking performance analyses for MMA2-2 and βMMA. The experiments have been performed considering (i) an equalized zero-forcing situation perturbed with random noise vector, (ii) a time-invariant channel, (iii) a time-varying channel (with a constant mean part and an autoregressive random part), and (iv) the effect of filter length on equalization performance.

4.1. Experiment I: considering zero-forcing solution

In this experiment, the elements of perturbation vector $\boldsymbol{q}_n$ are modeled as zero-mean wide-sense stationary and mutually uncorrelated. The corresponding positive definite autocorrelation matrix of $\boldsymbol{q}_n$ is obtained as $\boldsymbol{Q}=\sigma_q^2\boldsymbol{I}$ (where $\sigma_q=10^{-3}$).[3] The simulated EMSE has been obtained for equalizer lengths $N=7$ and $N=21$ for 16- and 64-QAM signals,[4] respectively. Each simulated trace is obtained by performing 100 independent runs where each run is executed for 5×10^3 iterations. Note that, due to assuming an already equalized scenario, we do not have to worry about the iterations required for successful convergence of the equalizer; thus the EMSE is computed for all iterations. The equalizer was initialized such that the first tap was unity and all taps were zero. The Monte-Carlo simulation requires to add the perturbation $\boldsymbol{q}_n$ directly in the weight update process. The weight update, in this experiment, is thus governed by

$$\boldsymbol{w}_n^o=\boldsymbol{w}_{n-1}^o+\mu\Phi(y_n)^*\boldsymbol{x}_n+\boldsymbol{q}_n \tag{37}$$

The terms containing the step-size μ and $\boldsymbol{q}_n$ contribute to acquisition and tracking errors [4], respectively. The rule (37) has been adopted in [4,15–17,31].

[3] Note that this modeling (*i.e.*, zero off-diagonal elements in $\boldsymbol{Q}$) is justified in the light of our analytical findings in Theorems 2 and 3 which imply that the EMSE depends neither on the individual diagonal elements nor the off-diagonal elements of matrix $\boldsymbol{Q}$, but rather depends on the trace of $\boldsymbol{Q}$ as denoted by P_q. In other words, given the sum of the mean square fluctuations of the elements of $\boldsymbol{q}_n$, the EMSE does not depend on the contribution of individual elements.

[4] In MMA2-2, $R_R=R_I$ are equal to 8.2 and 37 for 16- and 64-QAM, respectively. In βMMA, the parameter β is equal to 1.22 and 2.43 for 16- and 64-QAM, respectively.

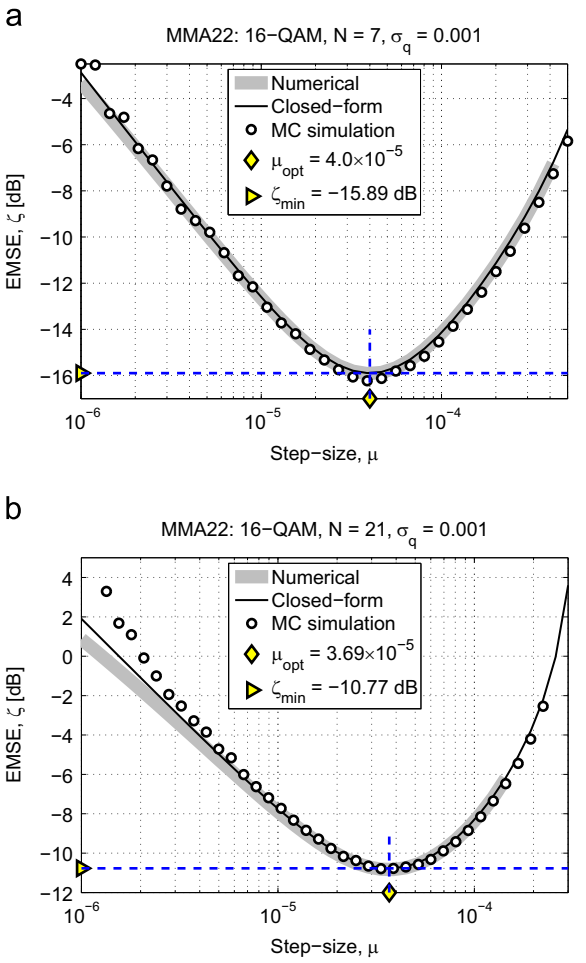

Fig. 3. EMSE traces for MMA2-2 for 16-QAM under zero-forcing scenario.

Since this experimental setup aims to evaluate both acquisition and tracking errors, the resulting EMSE is a convex downward function of step-size μ. Refer to Figs. 3 and 4 for the comparison of analytical and simulated EMSE of MMA2-2 equalizer. The legends 'Numerical' and 'Closed-from' refer to the solutions (21) and (T2.1), respectively. It is evident from this result that, for both QAM with smaller filter length (*i.e.*, $N=7$), the numerical, the closed-form and the simulated traces conform each other for all values of step-sizes. However, for larger filter length (*i.e.*, $N=21$), traces start deviating from each other for higher values of EMSE. Noticeably, for all four simulation cases, the analytically obtained minimum

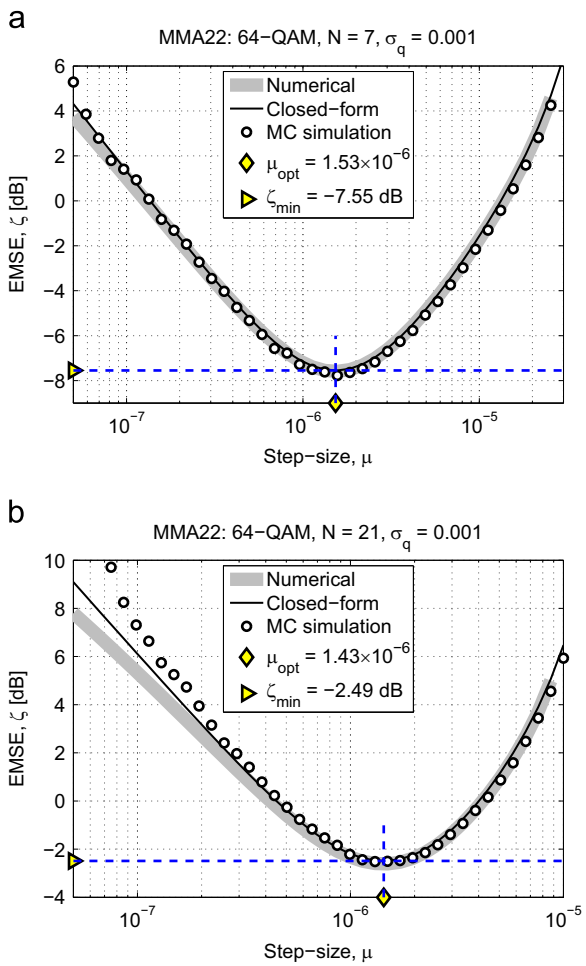

Fig. 4. EMSE traces for MMA2-2 for 64-QAM under zero-forcing scenario.

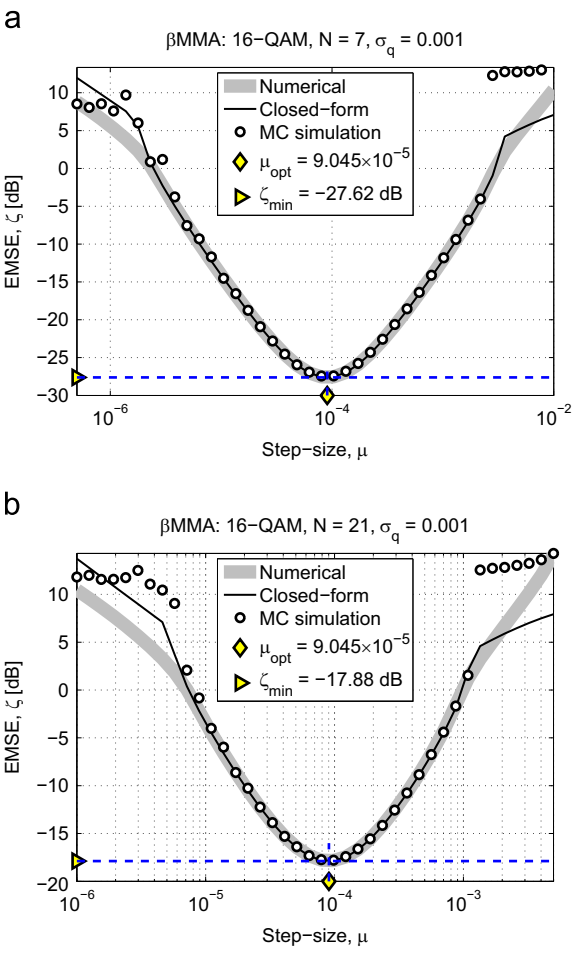

Fig. 5. EMSE traces for βMMA for 16-QAM under zero-forcing scenario.

EMSE ($\zeta_{\min}^{\mathrm{MMA2-2}}$) and the optimum step-size ($\mu_{\mathrm{opt}}^{\mathrm{MMA2-2}}$), as marked, respectively, with markers ▹ and ◊, are in good conformation with those obtained from simulation.

Next refer to Figs. 5 and 6 for the comparison of analytical and simulated EMSE of βMMA equalizer. The legends 'Numerical' and 'Closed-from' refer to the solutions (31) and (T3.1), respectively. It is evident from this result that, for both QAM with smaller filter length (*i.e.*, $N=7$), the numerical, the closed-form and the simulated traces conform each other for all values of step-sizes. However, for larger filter length (*i.e.*, $N=21$), traces start deviating from each other for higher values of EMSE. Noticeably, for all four simulation cases, the analytically obtained minimum EMSE ($\zeta_{\min}^{\beta\mathrm{MMA}}$) and the optimum step-size ($\mu_{\mathrm{opt}}^{\beta\mathrm{MMA}}$), as marked, respectively, with markers ▹ and ◊, match closely with those obtained from simulation.

To appreciate the lower EMSE exhibited by βMMA as compared to MMA2-2, we summarize the findings of above experiments for 16-QAM depicting the values of minimum EMSE achieved by both algorithms in Table 1. Note that (as expected) the numerical results are closer to those obtained by simulation.

Next we compare the abilities of MMA2-2 and βMMA to track the variations in non-stationary environments by obtaining the ratio of the minimum achievable steady-state EMSE as exhibited by MMA2-2 to that of βMMA. Mathematically, we compute the following ratio:

$$\eta := \frac{\zeta_{\min}^{\mathrm{MMA2-2}}}{\zeta_{\min}^{\beta\mathrm{MMA}}} \tag{38}$$

This ratio is obtained for 16-, 64- and 256-QAM and is summarized in Table 2 which indicates that the value of the minimum steady-state EMSE of βMMA is always less than that of MMA2-2 which reflects the superiority of βMMA over MMA2-2 for tracking variations in non-stationary environments.

4.2. Experiment II: equalizing time-invariant channel

In contrast to experiment I where we considered a zero-forcing scenario subject to random perturbation, here in this experiment, we consider an interfering $T/2$-spaced time-invariant channel whose impulse response is given by $\boldsymbol{h}_n = [0.1, 0.3, 1, -0.1, 0.5, 0.2]$ as used in [15,31]. In the sequel, we refer to this channel as `channel-1`. Since we

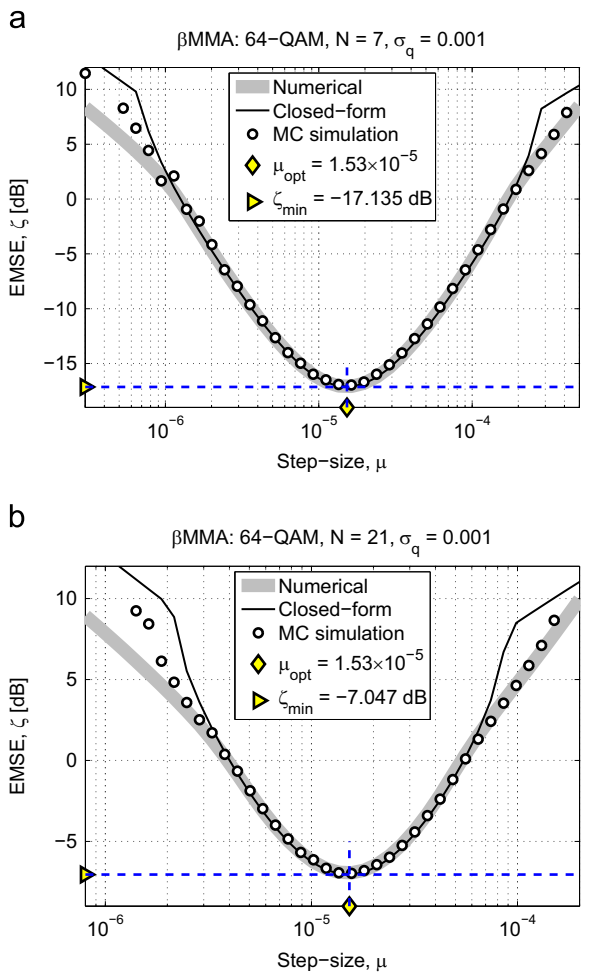

Fig. 6. EMSE traces for βMMA for 64-QAM under zero-forcing scenario.

Table 2
The ratio η for different QAM signals.

Equalizer taps	16-QAM (dB)	64-QAM (dB)	256-QAM (dB)
$N=7$	11.73	9.59	6.05
$N=21$	9.8	7.56	3.89

are not considering the random perturbation ($\sigma_q = 0$), the estimated EMSE comprises acquisition error only and is supposed to be a monotonic increasing function of step-size μ.

In this experiment, we consider a $T/2$-spaced equalizer and 16-QAM signaling for both MMA2-2 and βMMA. The equalizer is initialized such that the central tap is set to unity and the rest are set to zero. Refer to Fig. 7(a) for the comparison of analytical and simulated EMSE obtained for MMA2-2. The legends 'Numerical' and 'Closed-from' refer to the solutions (21) and (T2.1), respectively. Similarly, Fig. 7(b) depicts the comparison of analytical and simulated EMSE of βMMA equalizer in the presence of similar channel. The legends 'Numerical' and 'Closed-from' refer to the solutions (31) and (T3.1), respectively. It is evident from these results that the analytical and simulated traces conform closely with each other.

Note that the result in Fig. 7 also reveals that the steady-state EMSE (subject to successful convergence) of the larger filter will be higher than that of the smaller filter for the given value of step-size. Refer to Fig. 8 where the convergence traces of EMSE are depicted for two different filter lengths ($N=7$ and 21) for $\mu = 1 \times 10^{-4}$. The average values of the converged steady-state EMSE (for $N=7$ and 21) match closely with analytically estimated values obtained from Theorems 2 and 3.

4.3. Experiment III: equalizing time-varying channel

In contrast to experiments I and II, here we evaluate the performance analysis of the addressed equalizers in the presence of time-varying (TV) channel. A TV channel is usually modeled such that its autocorrelation properties correspond to wide-sense stationary and uncorrelated scattering (WSSUS) (as suggested by [36]). However, as reported in [37], a first-order (Gauss–Markov) autoregressive model is sufficient enough to model a slow-varying channel as given by $\boldsymbol{h}_n = \boldsymbol{h}_{\text{const}} + \boldsymbol{c}_n$, where $\boldsymbol{h}_n$ and $\boldsymbol{h}_{\text{const}}$ are as specified in Section 2, and $\boldsymbol{c}_n$ is the first-order Markov process as given by $\boldsymbol{c}_n = \alpha \boldsymbol{c}_{n-1} + \boldsymbol{d}_n$ where α is a constant, and the vector $\boldsymbol{d}_n$ is a zero-mean i.i.d. circular complex Gaussian process with correlation matrix $\boldsymbol{D}$[5].The matrix $\boldsymbol{D}$, due to WSSUS assumption, is diagonal and each of its diagonal element is σ_d^2. In the present scenario, we consider $\sigma_d^2 = 1 \times 10^{-3}, \alpha = 0.999$, and $\boldsymbol{h}_{\text{const}} = [1+0.2j, -0.2+0.1j, 0.1-0.1j]^T$ using a 7-tap baud-spaced equalizer with 16-QAM signaling. The ISI introduced by mean tap vector $\boldsymbol{h}_{\text{const}}$ is -11.72 dB. All simulation points were obtained by executing the program 10 times (or runs) with random and independent generation of transmitted data and channel perturbation. Each run was executed for as many iterations as required for the equalization of mean channel path $\boldsymbol{h}_{\text{const}}$. Once convergence is acquired, the equalizer is run for further 5000 iterations for the computation of steady-state value of EMSE.

Refer to Fig. 9 for the comparison of theoretical and simulated EMSE of MMA2-2 and βMMA equalizers. The legend 'Analysis' refers to the solutions (T2.1) and (T3.1) for MMA2-2 and βMMA equalizers, respectively. It is evident from the results that the theoretical and simulated EMSE traces conform each other. Note that the factor $P_q = E\|\boldsymbol{q}_n\|^2 = \text{trace}(\boldsymbol{Q})$ has been replaced with trace($\boldsymbol{D}$) in the evaluation of analytical EMSE. In the sequel, we refer to this TV channel ($\boldsymbol{h}_n$) as `channel-2`.

[5] For an AR(1) system, $\alpha = \mathcal{J}_0(2\pi f_D T)$, which makes the autocorrelation of the taps modeled by $\boldsymbol{c}_n = \alpha \boldsymbol{c}_{n-1} + \boldsymbol{d}_n$ equal the true autocorrelation at unit lag (where $\mathcal{J}_0$ is the zero-order Bessel function of the first kind, f_D is the Doppler rate and T is the baud duration). The parameter α determines the rate of the channel variation while the variances $\sigma_{d,i}^2$ of the ith entry of $\boldsymbol{d}_n$ determines the magnitude of the variation. So, α and $\sigma_{d,i}^2$ determine how "fast" and how "much" the time-varying part $c_{n,i}$ of each channel tap $h_{n,i}$ vary with respect to the known mean of that tap $h_{\text{const},i}$. The value of α can be estimated from the estimate of f_D. Similarly, given the average energy of the ith part of $\boldsymbol{c}_n$, $\text{E}\,|c_{n,i}|^2$, the value of $\sigma_{d,i}$ is evaluated as [37] $\sigma_{d,i} = |h_{\text{const},i}|^2 \sqrt{1-\alpha^2} \Big/ \sqrt{\text{E}|c_{n,i}|^2}$.

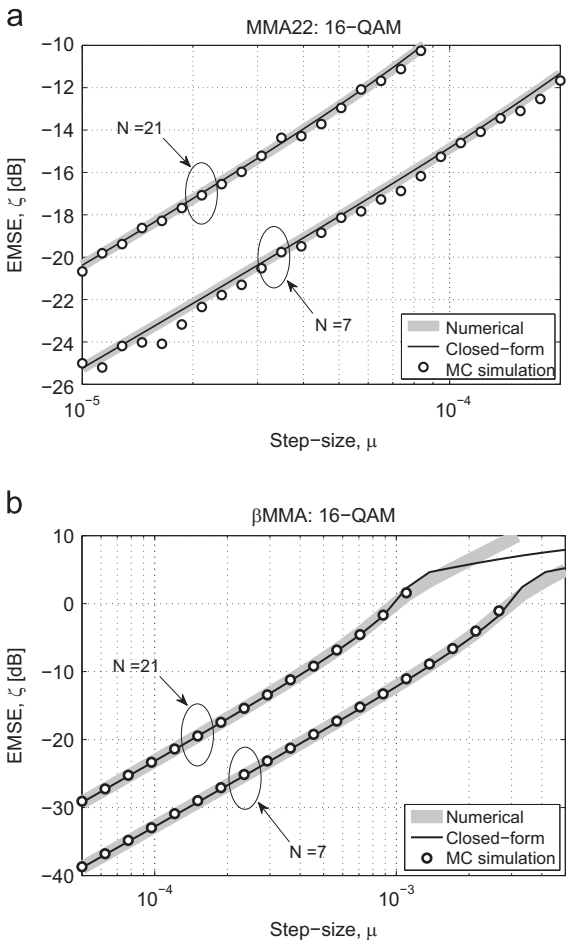

Fig. 7. EMSE traces for MMA2-2 and βMMA for 16-QAM for `channel-1`. All simulation points were obtained by executing the program 10 times (or runs) with random and independent generation of transmitted data. Each run was executed for as many iterations as required for the convergence. Once convergence is acquired, the equalizer is run for further 5000 iterations for the computation of steady-state value of EMSE. So $10 \times 5000 = 5 \times 10^4$ samples were used in the computation of each EMSE point. Note that, for 16-QAM signaling on `channel-1`, MMA2-2 ($\mu = 3 \times 10^{-5}$) and βMMA ($\mu = 4 \times 10^{-4}$) required nearly 7000 and 1500 iterations (on the average), respectively, to acquire same (-20 dB) EMSE floor.

4.4. Experiment IV: effect of filter-length on EMSE

In all previous experiments, we have considered different channel conditions where the effect of filter-length on equalization capability has not been taken in consideration. It is quite obvious that a reasonable filter-length is required to equalize successfully a propagation channel. An insufficient filter-length, therefore, introduces an additional distortion which have not been considered in Theorems 2 and 3. However, as mentioned in [3], the distortive effect of insufficient filter-length may easily be incorporated (in the EMSE expressions) as an additive term; the total EMSE, which we denote as TEMSE, is thus given as follows:

$$\text{TEMSE} = \underbrace{\lim_{n\to\infty} \mathrm{E}|e_{a,n}|^2}_{=\zeta} + \underbrace{\mathrm{E}|a_n|^2 \|\mathcal{H}\boldsymbol{w}^{o*} - \boldsymbol{e}\|^2}_{=\chi} \tag{39}$$

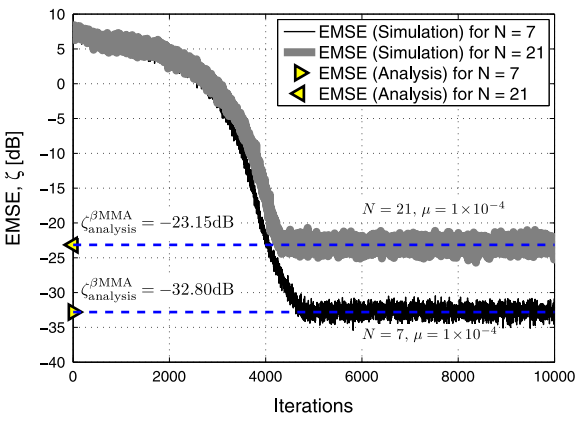

Fig. 8. Transient EMSE traces for βMMA for 16-QAM on `channel-1`. Note that the performance of equalizer is far better with (N=7) than (N=21); this behavior is explained in Experiment IV.

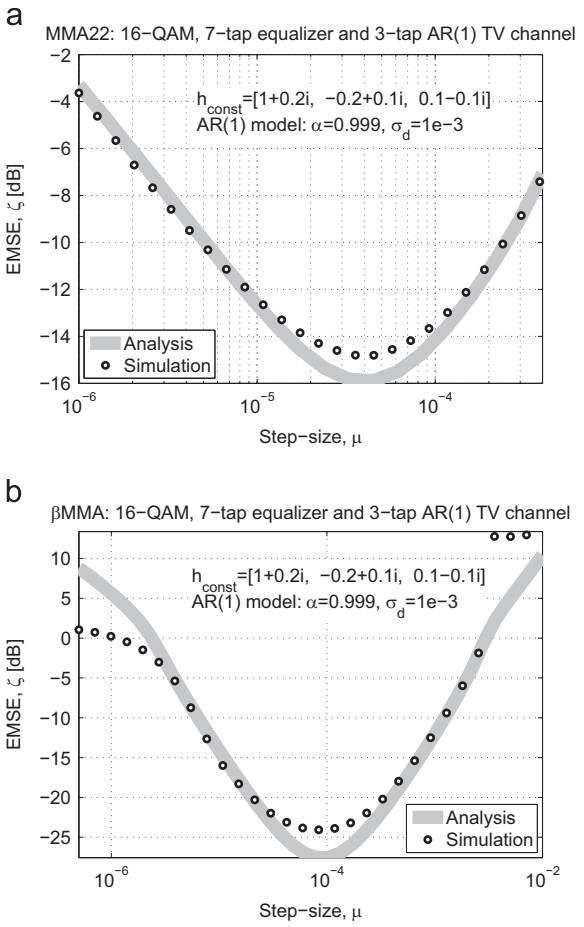

Fig. 9. EMSE traces for MMA2-2 and βMMA with 16-QAM signaling for `channel-2`. With f_{DT}=0.01 and unit lag, we have α=0.999.

where ζ is EMSE as we obtained in Theorems 2 and 3, and χ is the additional squared error contributed by the (insufficient) filter-length. The vector $\boldsymbol{w}^o$ is the zero-forcing solution, $\mathcal{H}$ is the channel matrix, and $\boldsymbol{e}$ is the

overall idealistic (single-spike) channel-equalizer impulse response as defined in Section 2.

In Section 4.2, we have observed that the EMSE, ζ, is proportional to filter-length for the given step-size. The parameter χ on the other hand decreases with filter-length.[6] In our simulation, the value of optimal weight vector $\boldsymbol{w}^o$ is obtained as $\boldsymbol{w}^o = \texttt{pinv}(\mathcal{H})\boldsymbol{e}$ where $\texttt{pinv}(\cdot)$ is the MATLAB function for the evaluation of pseudo-inverse. The TEMSE as expressed in (39) is a convex downward function of filter-length. Evaluating TEMSE for different filter-lengths can provide us with the optimal value of filter-length required to equalize the given channel and given step-size. In this simulation, we have considered a voice-band telephone channel $\boldsymbol{h}_n = [-0.005 - 0.004j, 0.009 + 0.03j, -0.024 - 0.104j, 0.854 + 0.52j, -0.218 + 0.273j, 0.049 - 0.074j, -0.016 + 0.02j]$ [38] and 16-QAM signaling. The ISI introduced by this channel is -8.44 dB. In the sequel, we refer to this channel as `channel-3`.

All simulation points were obtained by executing the program 10 times (or runs) with random and independent generation of transmitted data. Each run was executed for as many iterations as required for the convergence. Once convergence is acquired, the equalizer is run for further 5000 iterations for the computation of steady-state value of EMSE. In Fig. 10, we depict analytical and simulated TEMSE obtained as a function of filter-length for the given step-sizes for both MMA2-2 and βMMA. Both analytical and simulated TEMSE are found to be in close agreement.

5. Conclusion

In this paper, we studied the steady-state mean square tracking performance of two popular equalizers, MMA2-2 and βMMA, by exploiting the fundamental variance relation. Analytical expressions for the steady-state EMSE were evaluated and validated by computer simulations. For this study, we conclude the following:

1. The fundamental variance relation described in Section 3 is useful for the analysis of steady-state performance of (gradient-based) adaptive equalizers. By using this relation, we have been able to obtain the EMSE of MMA2-2 and βMMA in closed-form. We have validated our analytical findings under zero-forcing situation, stationary and non-stationary channel environments.
2. βMMA is superior to MMA2-2 equalizer in equalizing channel with square-QAM signaling. Under similar environmental conditions, the minimum EMSE of MMA2-2 is found to be in excess of 6–12 dB as compared to that of βMMA.
3. The so-called total EMSE (TEMSE) has been found to be useful in determining the optimum lengths of the addressed equalizers for underlying channels and given values of step-sizes. Our experiments have indicated that the optimum lengths for MMA2-2 equalizer and βMMA equalizers for a typical (7-tap) voice-band are between 7 and 15 depending upon the step-size.

[6] The actual expression of χ (as denoted by D_f in [3, Eq. 4.8.24]) contains an equalizer solution (as denoted by $\overline{\boldsymbol{\theta}}$) that also depends on blind equalization error-function. However, we have observed that the exact value of $\overline{\boldsymbol{\theta}}$ is very close to $\mathcal{H}^+\boldsymbol{e}$ for both MMA2-2 and βMMA where $(\cdot)^+$ denotes pseudo-inverse. So, in this work, we have replaced the exact expression of $\overline{\boldsymbol{\theta}}$ with its simplified form $\boldsymbol{w}^{o*} = \mathcal{H}^+\boldsymbol{e}$ and our simulation findings (as depicted in Fig. 10) validate that this simplification is reasonable.

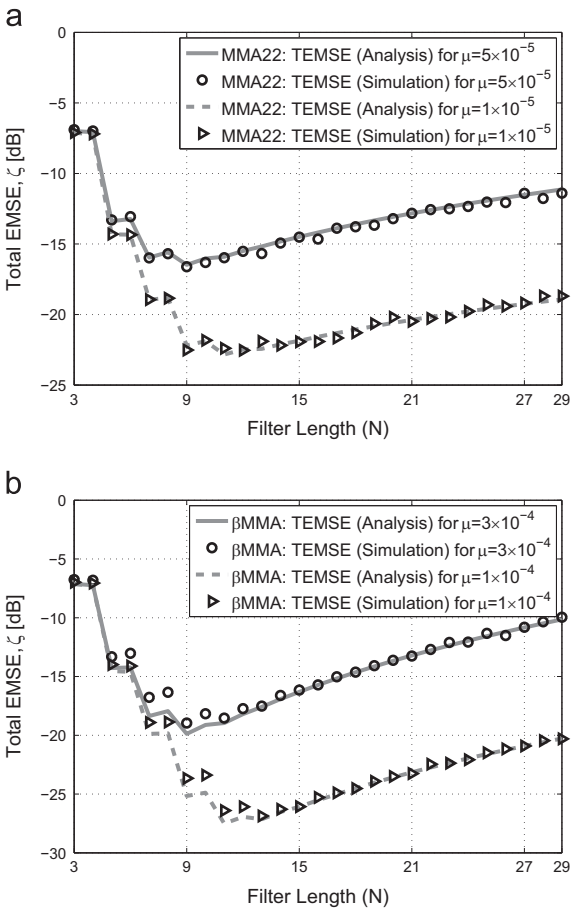

Fig. 10. EMSE traces considering the effect of filter-length for `channel-3`. (a) The optimal filter-length for MMA2-2 is found to be 9 for both 1×10^{-5} and 5×10^{-5}. (b) The optimal filter-length for βMMA is found to be between 9 and 11 for 3×10^{-4} and 1×10^{-4}, respectively.

References

[1] S. Haykin, Blind Deconvolution, PTR Prentice Hall, Englewood Cliffs, 1994.
[2] R. Johnson Jr., P. Schniter, T. Endres, J. Behm, D. Brown, R. Casas, Blind equalization using the constant modulus criterion: a review, Proc. IEEE 86 (10) (1998) 1927–1950.
[3] Z. Ding, Y. Li, Blind Equalization and Identification, Marcel Dekker, Inc., New York, Basel, 2001.
[4] A.H. Sayed, Fundamentals of Adaptive Filtering, John Wiley & Sons, Hoboken, New Jersey, 2003.
[5] D. Godard, Self-recovering equalization and carrier tracking in two-dimensional data communication systems, IEEE Trans. Commun. 28 (11) (1980) 1867–1875.
[6] J. Treichler, M. Larimore, New processing techniques based on the constant modulus adaptive algorithm, IEEE Trans. Acoust. Speech Signal Process. 33 (2) (1985) 420–431.

[7] S. Abrar, A. Zerguine, A.K. Nandi, Adaptive blind channel equalization, in: C. Palanisamy (Ed.), Digital Communication, InTech Publishers, Rijeka, Croatia, 2012. (Chapter 6).
[8] K. Wesolowski, Analysis and properties of the modified constant modulus algorithm for blind equalization, Eur. Trans. Telecommun. 3 (3) (1992) 225–230.
[9] K.N. Oh, Y.O. Chin, Modified constant modulus algorithm: blind equalization and carrier phase recovery algorithm, Proc. IEEE Globcom (1995) 498–502.
[10] J. Yang, J.-J. Werner, G.A. Dumont, The multimodulus blind equalization and its generalized algorithms, IEEE J. Sel. Areas Commun. 20 (5) (2002) 997–1015.
[11] J.-T. Yuan, K.-D. Tsai, Analysis of the multimodulus blind equalization algorithm in QAM communication systems, IEEE Trans. Commun. 53 (9) (2005) 1427–1431.
[12] X.-L. Li, W.-J. Zeng, Performance analysis and adaptive newton algorithms of multimodulus blind equalization criterion, Signal Process. 89 (11) (2009) 2263–2273.
[13] J.-T. Yuan, T.-C. Lin, Equalization and carrier phase recovery of CMA and MMA in blind adaptive receivers, IEEE Trans. Signal Process. 58 (6) (2010) 3206–3217.
[14] I. Fijalkow, C.E. Manlove, R. Johnson Jr., Adaptive fractionally spaced blind CMA equalization: excess MSE, IEEE Trans. Signal Process. 46 (1) (1998) 227–231.
[15] J. Mai, A.H. Sayed, A feedback approach to the steady-state performance of fractionally spaced blind adaptive equalizers, IEEE Trans. Signal Process. 48 (1) (2000) 80–91.
[16] N.R. Yousef, A.H. Sayed, A unified approach to the steady-state and tracking analyses of adaptive filters, IEEE Trans. Signal Process. 49 (2) (2001) 314–324.
[17] S. Abrar, A. Ali, A. Zerguine, A.K. Nandi, Tracking performance of two constant modulus equalizers, IEEE Commun. Lett. 17 (5) (2013) 830–833.
[18] S. Abrar, A.K. Nandi, Adaptive minimum entropy equalization algorithm, IEEE Commun. Lett. 14 (10) (2010) 966–968.
[19] N. Xie, H. Hu, H. Wang, A new hybrid blind equalization algorithm with steady-state performance analysis, Dig. Signal Process. 22 (2) (2012) 233–237.
[20] T. Thaiupathump, L. He, S.A. Kassam, Square contour algorithm for blind equalization of QAM signals, Signal Process. 86 (11) (2006) 3357–3370.
[21] S.A. Sheikh, P. Fan, New blind equalization techniques based on improved square contour algorithm, Dig. Signal Process. 18 (5) (2008) 680–693.
[22] S.A. Sheikh, P. Fan, Two efficient adaptively varying modulus blind equalizers: AVMA and DM/AVMA, Dig. Signal Process. 16 (6) (2006) 832–845.
[23] S. Abrar, A.K. Nandi, Adaptive solution for blind equalization and carrier-phase recovery of square-QAM, IEEE Signal Process. Lett. 17 (9) (2010) 791–794.
[24] S. Bellini, Bussgang Techniques for Blind Deconvolution and Equalization, Blind Deconvolution, Prentice Hall, Upper Saddle River, N.J, 1994.
[25] K. Wesolowski, Self-recovering adaptive equalization algorithms for digital radio and voiceband data modems, in: Proceedings of European Conference on Circuit Theory and Design, 1987, pp. 19–24.
[26] S. Abrar, A.K. Nandi, Blind equalization of square-QAM signals: a multimodulus approach, IEEE Trans. Commun. 58 (6) (2010) 1674–1685.
[27] S. Abrar, S.I. Shah, New multimodulus blind equalization algorithm with relaxation, IEEE Signal Process. Lett. 13 (7) (2006) 425–428.
[28] C. Meng, J. Tuqan, Z. Ding, A quadratic programming approach to blind equalization and signal separation, IEEE Trans. Signal Process. 57 (6) (2009) 2232–2244.
[29] T.Y. Al-Naffouri, A.H. Sayed, Adaptive filters with error nonlinearities: mean-square analysis and optimum design, EURASIP J. Appl. Signal Process. 1 (2001) 192–205.
[30] D. Dohono, On minimum entropy deconvolution, in: Proceedings of the Second Applied Time Series Symposium, vol. 1, 1980, pp. 565–608.
[31] M.T.M. Silva, M.D. Miranda, Tracking issues of some blind equalization algorithms, IEEE Signal Process. Lett. 11 (9) (2004) 760–763.
[32] S. Vaseghi, Advanced Digital Signal Processing and Noise Reduction, John Wiley & Sons, West Sussex, England, 2008.
[33] T.Y. AlNaffouri, A.H. Sayed, Transient analysis of adaptive filters with error nonlinearities, IEEE Trans. Signal Process. 51 (3) (2003) 653–663.
[34] O. Dabeer, E. Masry, Convergence analysis of the constant modulus algorithm, IEEE Trans. Inf. Theory 49 (6) (2003) 1447–1464.
[35] A. Benveniste, M. Goursat, G. Ruget, Robust identification of a nonminimum phase system: blind adjustment of a linear equalizer in data communications, IEEE Trans. Autom. Control 25 (3) (1980) 385–399.
[36] P. Bello, Characterization of randomly time-variant linear channels, IEEE Trans. Commun. Syst. 11 (4) (1963) 360–393.
[37] C. Komninakis, C. Fragouli, A.H. Sayed, R.D. Wesel, Multi-input multi-output fading channel tracking and equalization using Kalman estimation, IEEE Trans. Signal Process. 50 (5) (2002) 1065–1076.
[38] G. Picchi, G. Prati, Blind equalization and carrier recovery using a "stop-and-go" decision-directed algorithm, IEEE Trans. Commun. 35 (9) (1987) 877–887.